

Influence of Slot Parameters on the Structure Performance of Slotted Tunnels under the Internal Chemical Explosion

Zhang Yu^a, Yuanxue Liu^{*a}, Runze Wu^a, Jichang Zhao^a, Yizhong Tan^b

^a Chongqing Key Laboratory of Geomechanics & Geoenvironmental Protection, Dept. of Civil Engineering, Logistical Engineering University, Chongqing 401311, China;

^b PLA Engineering College, Xuzhou, China.
 357202780@qq.com

The chemical explosion is a complicated process with the coupling action of the temperature field and pressure field. Under the internal chemical explosion, tunnels with different slot parameters such as the slot area ratio and the slot depth have different structure performance. In this paper, the influence of slot parameters on the structure performance of slotted tunnels under the internal chemical explosion was studied numerically. 3 schemes were conducted to obtain the structure performance of slotted tunnels, which were different slot area ratios, different slot depths and their different combinations respectively. Based on the finite element analysis software LS-DYNA, the peak vertical acceleration and the peak maximum principal stress of the tunnel roof under different slot parameters were calculated to obtain the structure performance, which can help provide a reference for the explosion resisting design of slotted tunnels.

1. Introduction

In recent years, as one of the main means of terrorist activities, the world's explosive attacks have caused a significant threat to the security of the engineering structure and personnel. For example, consecutive violent explosions occurred to 6 subway stations in London on July 7, 2005. The explosion caused the closure of 13 subway lines, with 56 people dead (Hunter, 2005, Qu and Li, 2012). The chemical explosion is a complicated process, and the coupling effect of the temperature field and pressure field is involved in the process. Under the internal chemical explosion, the structure performance of slotted tunnels is affected by the thermodynamic properties of the air and structure. The air flow patterns strongly depend on the air supply and exhaust outlet location (Balocco et al., 2015). The thermodynamic property of concrete and the temperature field were analyzed by Zhang (2015). At present, the shock wave propagation, structural dynamic response and explosion protection measures are 3 main aspects for structural explosion analysis. A series of internal explosion model tests on different kinds of tunnels and other underground structures were carried out and the curves of the overpressure with dynamic time for underground structures were obtained under the internal explosion (Smith and Mays, 1992). Wu et al. (2010) studied the explosion response of the right angle turning tunnel using LS-DYNA based on the computed results and the experimental results. The transmission of flames and explosion pressure waves in pipes under the application of systems for explosion isolation with explosion venting was studied by Sippel et al. (2016), which can also be applied to tunnels.

For slotted tunnels, shown in Figure 1, the internal chemical explosion can result in the different responses according to different slot parameters, which hasn't been studied by scholars. In this paper, the influence of slot parameters on the structure performance of slotted tunnels under the internal chemical explosion was studied numerically. 3 schemes of different slot area ratios, different slot depths and their different combinations were conducted to obtain the structure performance of slotted tunnels. The peak vertical acceleration and the peak maximum principal stress of the tunnel roof under different slot parameters were calculated to get the structure performance.

2. Numerical model and material parameters

2.1 Numerical model

A rectangular tunnel is adopted in the numerical analysis with the clear width of 5m, clear height of 4m, roof thickness of 0.5m, wall thickness of 0.5m and floor thickness of 0.2m. The structure is buried at the depth of 10m, and the surrounding rock is the granite. The explosive is a cubic TNT charge of 20kg, and the distance from the charge center to the ground is 1.2m, initiating in the vertical axis of the structure. Considering the symmetry of the structure and explosive, only 1/4 model is needed in the calculation. The numerical model has a total height of 21.2m, a total width of 8m, and a total length of 50m. The size and the boundary condition of the model are listed in Figure 2.

Three kinds of schemes are designed in the calculation. In scheme 1, the slot depth keeps constant as 1m, and the slot area ratio is 0%, 4.2%, 8.3%, 16.7% and 33.3% respectively. In scheme 2, the slot depth is 0m, 0.5m, 1m, 2m, 3m and 5.5m respectively, while the slot area ratio keeps constant as 33.3%. In scheme 3, three combinations of the slot area ratio and slot depth under the same excavation volume are researched, and the combinations are as follows, 33.3% slot area ratio and 0.5m slot depth, 16.7% slot area ratio and 1m slot depth, 8.3% slot area ratio and 2m slot depth. Points and elements in the longitudinal axis of the roof are chosen to monitor the vertical acceleration and maximum principle stress, and the monitoring positions with the unit of cm are shown in Figure 3.

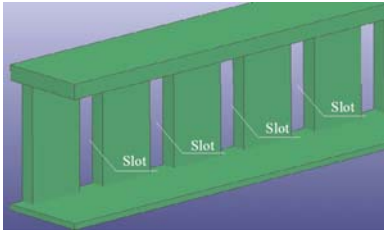


Figure 1: Diagram of half the slotted tunnel

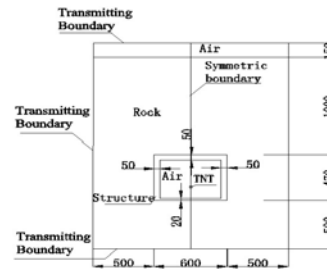


Figure 2: Size and boundary conditions of the tunnel model (unit: cm)

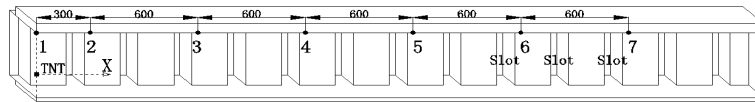


Figure 3: Diagram of the monitoring positions on the longitudinal axis of tunnel roof (half the tunnel)

2.2 Material parameters

The MAT_HIGH_EXPLOSIVE_BURN constitutive model and EOS_JWL state equation are adopted for TNT, and parameters are in Table 1 (Liu et al., 2007). The air adopts the MAT_NULL constitutive model and EOS_LINEAR_POLYNOMIAL state equation and parameters are listed in Table 2 (Zhang et al., 2009). The MAT_JOHNSON_HOLMQUIST_CONCRETE constitutive model is used for the structure and material parameters are based on literature (Holmquist and Johnson, 1993), with the reinforcement ratio of 1.5% considered in this case, shown in Table 3. Data in the tables obey the unit system of cm-g-us. The granite adopts the MAT_PLASTIC_KINEMATIC plastic dynamics model, and material parameters are listed in Table 4 (Bai, 2005).

Table 1: Parameters for TNT

		MAT_HIGH_EXPLOSIVE_BURN				
TNT		RO	D	PCJ		
		1.63	0.693	0.21		
		EOS_JWL				
	A	B	R1	R2	OMEG	E0
	3.71	0.0323	4.15	0.95	0.38	0.08

Table 2: Parameters for the air

MAT_HIGH_EXPLOSIVE_BURN						
RO	PC	MU				
0.00129	0	0				
EOS_LINEAR_POLYNOMIAL						
C0	C1	C2	C3	C4	C5	
-1.00E-06	0	0	0	0.4	0.4	

Table 3: Parameters for the structure

MAT_JOHNSON_HOLMQUIST_CONCRETE						
RO	G	A	B	C	N	FC
2.519	0.16	0.79	1.6	0.007	0.61	0.00054
T	EFMIN	SFMAX	PC	UC	PL	UL
5.40E-05	0.01	7	0.00018	0.00104	0.008	0.1
D1	D2	K1	K2	K3		
0.04	1	0.85	-1.71	2.08		

Table 4: Parameters for the granite

MAT_PLASTIC_KINEMATIC						
RO	E	PR	SIGY	ETAN	FS	
2.6	0.55	0.27	0.00117	0	0.06	

3. Verification of the calculation accuracy

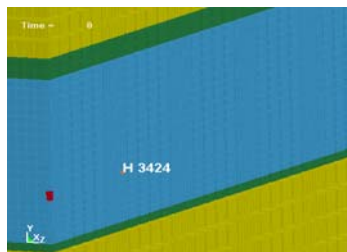
Through the analysis on explosion tests, Henrych obtained the following empirical formula of shock wave attenuation in free air (Henrych, 1987).

$$\Delta p_{\phi} = \frac{14.0717}{\bar{R}} + \frac{5.5397}{\bar{R}^2} - \frac{0.3572}{\bar{R}^3} + \frac{0.00625}{\bar{R}^4}, \quad 0.05 \leq \bar{R} \leq 0.3$$

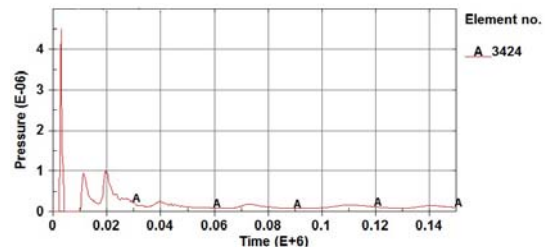
$$\Delta p_{\phi} = \frac{6.1938}{\bar{R}} - \frac{0.3262}{\bar{R}^2} + \frac{2.1324}{\bar{R}^3}, \quad 0.3 \leq \bar{R} \leq 1 \quad (1)$$

$$\Delta p_{\phi} = \frac{0.662}{\bar{R}} + \frac{4.05}{\bar{R}^2} + \frac{3.288}{\bar{R}^3}, \quad 1 \leq \bar{R} \leq 10$$

where, Δp_{ϕ} is the peak overpressure at the wave front (kg/cm^2), and \bar{R} is the proportional explosion distance obeying $\bar{R} = R / \sqrt[3]{W}$, in which R is the distance from the charge centre to the monitoring point and W is the mass of the explosive. Equation (1) can also be used in the air explosion in a tunnel when the monitoring point is relatively near the explosive, for that in this condition the first peak overpressure in the curve of overpressure with time must be in accordance with Equation (1) and the reflected wave only influence the overpressure after the first peak. Particle H with a distance of 3.36m from the explosive center is chosen to verify the accuracy of the simulation, shown in Figure 4. The peak overpressure by Henrych formula is 0.49 MPa, while the first peak overpressure by the simulation is 0.45 MPa, and the relative error is 8.2% within the allowable range.



(a)



(b)

Figure 4: Layout of monitoring point H and curve of the overpressure with time(unit system of g-cm-us)

4. Numerical results and analysis

4.1 Influence of the slot area ratio

Scheme 1 is adopted in this section. The variations of the peak vertical acceleration for monitoring positions of the roof with the explosion distance under different slot area ratios are shown in Figure 5. With the increase of the explosion distance, the peak vertical acceleration for monitoring positions of the roof has the trends of decrease-increase-decrease. The reason of the increase trend is that the surface wave is gradually formed in the roof surface of the tunnel in the explosion (He et al., 2002). Within the explosion distance of 15m, the peak vertical accelerations under all conditions have no obvious difference. When the explosion distance is out of 15m, the peak vertical accelerations under the slot conditions are generally lower than that of the condition without slots. Beyond the distance of 15m, the specific change rule between the peak vertical accelerations and the slot area ratios is hard to obtain, and this is because that the peak vertical accelerations for monitoring positions of the roof are determined by the overpressure of the shock wave and the supporting conditions of the side wall.

The variations of the peak maximum principle stress for monitoring positions of the roof with the explosion distance under different slot area ratios are shown in Figure 6. The maximum principal stresses for monitoring positions of the roof decrease generally with the increase of the slot area ratio, which indicates that the number of dangerous cross sections can be effectively reduce. It can be deduced that there may be a limit for the slot area ratio, and the peak maximum principle stress of the roof is likely to become larger generally if the slot area ratio exceeds the limit.

Combined with the peak vertical acceleration and peak maximum principal stress of all monitoring points, it can be concluded that when the slot area ratio is within a certain range, the dynamic response of the structure generally gets less intense with the increase of the slot area ratio under the same slot depth. Of course, it can be deduced that there may be a limit for the slot area ratio, and the dynamic response of the structure is likely to become more intense if the slot area ratio exceeds the limit.

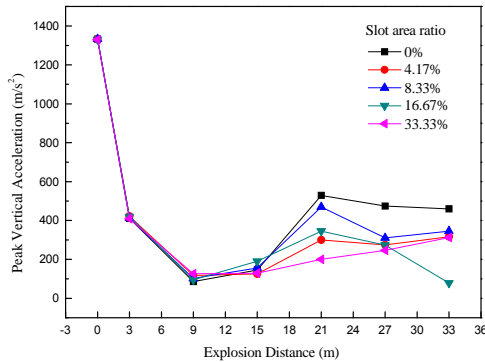


Figure 5: Variations of the peak vertical acceleration for monitoring positions with the explosion distance under different slot area ratios

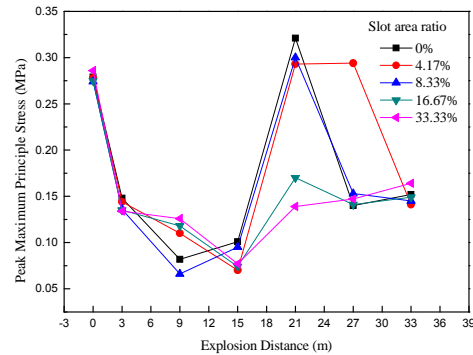


Figure 6: Variations of the peak maximum principle stress for monitoring positions with the explosion distance under different slot area ratios

4.2 Influence of the slot depth

Scheme 2 is adopted in this section. Variations of the peak vertical acceleration for monitoring positions of the roof with the explosion distance under different slot depths are shown in Figure 7. The peak vertical accelerations under the slot depth of 0.5m, 1m, 2m, 3m and 5.5m are generally lower than that of the condition without slots. The peak vertical acceleration curves show a trend of decrease-increase-decrease with the explosion distance on the whole. In a certain depth range (3m in this case), the peak vertical acceleration generally gets smaller with the increase of the slot depth. For instance, in the position of 33m explosion distance, the peak vertical acceleration for the slot depth of 0m, 0.5m, 1m, 2m and 3m is $459 m/s^2$, $287 m/s^2$, $317 m/s^2$, $42.1 m/s^2$, $36.8 m/s^2$ respectively. But when the slot depth exceeds the range (3m in this case), with the increase of the slot depth, the peak vertical acceleration of each monitoring point would gradually increase generally. For example, in the position of 33m explosion distance, the peak vertical acceleration for the slot depth of 5.5m increases to $336 m/s^2$. The reason for this phenomenon is that when the slot depth is too large, the total space of underground structures will increase so remarkably that the load of the surrounding rock on the structure will increase a lot, which results in the lower stability of the whole system of the structure and rock.

Variations of the peak maximum principle stress for monitoring positions of the roof with the explosion distance under different slot depths are shown in Figure 8. The variation principle of the peak maximum principal stress with the explosion distance is approximately the same as the change trend of the peak vertical acceleration. Combined with the peak vertical acceleration and peak maximum principal stress of all monitoring points, it can be concluded that the peak vertical acceleration and peak maximum principal stress of monitoring positions under the slot depth of 3m are generally less than that of the other slot depth conditions. The structure with the slot depth of 3m is more conducive to the structural safety under the condition of explosion in this case.

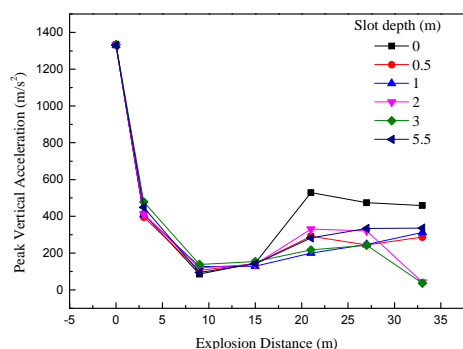


Figure 7: Variations of the peak vertical acceleration for monitoring positions with the explosion distance under different slot depths

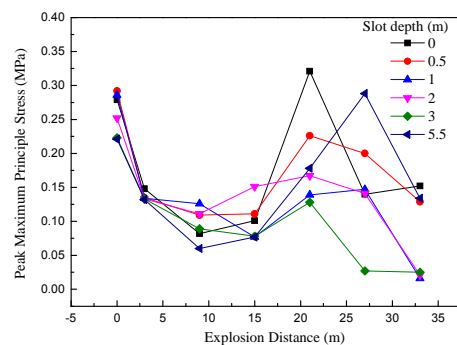


Figure 8: Variations of the peak maximum principle stress for monitoring positions with the explosion distance under different slot depths

4.3 Influence of the combinations of the slot area ratio and depth

The combinations of the slot area ratio and depth under the same excavation volume in scheme 3 are considered in this part. Variations of the peak vertical acceleration for monitoring positions of the roof with the explosion distance under different combinations are shown in Figure 9. The peak vertical accelerations have no obvious difference within the explosion distance of 25m, because the vibration characteristics of the structure are affected by the shock wave overpressure, the slot area ratio and the slot depth. Variations of the peak maximum principle stress for monitoring positions of the roof with the explosion distance under different combinations are shown in Figure 10. In the combination of 33.3% slot area ratio and 0.5m slot depth, the maximum principal stresses of the monitoring points in the roof are generally larger than the other two combinations. It also shows that under the condition of equal excavation volume, the tensile stress on the roof of the structure will get greater if the slot area ratio is too large, which is bad to the structure safety. The reason of this phenomenon is that when the total volume of slots is equal, if the slot area ratio is too large, the bearing condition of the structure will be weakened heavily. On the contrary, the increase of the slot depth will not generally weaken the bearing condition.

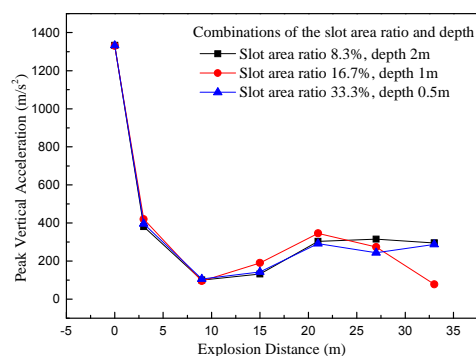


Figure 9: Variations of the peak vertical acceleration for monitoring positions with the explosion distance under different combinations

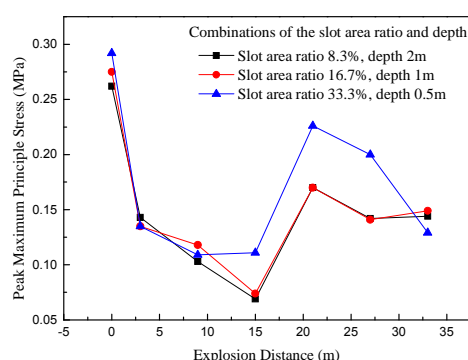


Figure 10: Variations of the peak maximum principle stress for monitoring positions with the explosion distance under different combinations

5. Conclusions

In this paper, the influence of the different slot parameters on the structure performance of slotted tunnels was studied under the internal chemical explosion. The peak vertical acceleration and the peak maximum principal stress of the tunnel roof under different slot parameters were calculated to obtain the explosion resisting performance of the tunnel. The main conclusions are as follows:

1. The peak vertical acceleration of monitoring positions in the tunnel roof has the trend of decrease-increase-decrease. The reason of the increase trend is that the surface wave is gradually formed in the roof under the internal chemical explosion.
2. Under the condition of constant slot depth, when the slot area ratio is within a certain range, the maximum principal stresses for monitoring positions of the roof decrease generally with the increase of the slot area ratio, which indicates that the number of dangerous cross sections can be effectively reduce. When the slot area ratio is out of the range, the peak maximum principle stress of the roof is likely to become larger generally.
3. Under the condition of constant slot area ratio, within a certain depth range, the peak vertical acceleration and the peak maximum principal stress of the monitoring positions in the tunnel roof generally get smaller with the increase of the slot depth. Beyond the range, the peak vertical acceleration and peak maximum principal stress would increase generally with the increase of the slot depth.
4. Under the condition of equal excavation volume, the maximum principal stresses of monitoring positions on the roof will get greater if the slot area ratio is too large, which is harmful to the structure safety. On the contrary, the increase of the slot depth will not generally weaken the safety of the structure.

Acknowledgements

We gratefully acknowledge the support from Chongqing Graduate Student Innovation Project under grant No.CYB14103, Chongqing Research Program of Basic Research and Frontier Technology under grant No.cstc2014jcyjA30015, No.cstc2015 jcyjBX0073, No.cstc2014jcyjA30014, Science and Technology Project of Land Resources and Real Estate Management Bureau of Chongqing Government under grant No.CQGT-KJ-2014052.

Reference

- Bai J.Z., 2005, Theoretical Foundation and the Case Analysis of LS-DYNA3D, Science Press, Beijing, China.
- Balocco C., Petrone G., Cammarata G., 2015, Thermo-fluid dynamics analysis and air quality for different ventilation patterns in an operating theatre, *International Journal of Heat and Technology*, 33, 4, 25-32, DOI: 10.18280/ijht.330404
- He X., Wu X.Y., Ren H.Q., Li M.S., Wang L.Z., Qu J.B., Pang W.B., 2002, Experimental research on the macro failure phenomenon and blast wave propagation in tunnels, *Proceedings of 2nd National Conference on Experimental Techniques for Explosive Mechanics*, China, 19-28.
- Henrych J., 1987, *Explosion Dynamics and Its Application*, Xiong, J.G., tran, Science Press, Beijing, China.
- Holmquist T.J., Johnson G.R., 1993, A computational constitutive model for concrete subjected to large strains, high strain rates, and high pressures, 14th International Symposium on Ballistics, Quebec, Canada, 591-600.
- Hunter P., 2005, London terrorist attacks heat up identity card debate and highlight uncertainties over their efficacy, *Computer Fraud & Security*, 5, 4-5, DOI: 10.1016/S1361-3723(05)70230-X
- Liu J.B., Du Y.X., Yan Q.S., 2007, Dynamic response of underground box structures subjected to blast load, *Journal of PLA University of Science and Technology*, 8, 5, 520-524.
- Qu S.S., Li Z.X., 2012, Dynamic response and damage analysis of a subway station structure due to internal explosion, *Journal of Tianjin University*, 45, 4, 285-291, DOI: 10.3969/j.issn.0493-2137.2012.04.002
- Sippel M., Schepp P., Hesener U., 2016, New findings for the application of systems for explosion isolation with explosion venting, *Chemical Engineering Transactions*, 48, 529-534, DOI: 10.3303/CET1648089.
- Smith P.D., Mays G.C., 1992, Small scale models of complex geometry for blast overpressure assessment, *International Journal of Impact Engineering*, 12, 3, 345-360. DOI: 10.1016/0734-743X(92)90112-7
- Wu S.Y., Zhang D., Lu F.Y., 2010, Study on propagation laws of blast in tunnels, *Chinese Journal of Underground Space and Engineering*, 6, 2, 396-399, DOI: 10.3969/j.issn.1673-0836.2010.02.033
- Zhang H.Y., 2015, Thermodynamic property of concrete and temperature field analysis of the base plate of intake tower during construction period, *International Journal of Heat and Technology*, 33, 1, 145-154, DOI: 10.18280/ijht.330120.
- Zhang X.H., Duan Z.D., Zhang C.W., 2009, Shock responses of steel frame structure near the ground explosion, *Journal of Earthquake Engineering and Engineering Vibration*, 29, 4, 70-76.